J|A|C|S
ARTICLES
Published on Web 11/14/2003

Molecular Quantum Cellular Automata Cells. Electric Field Driven Switching of a Silicon Surface Bound Array of Vertically Oriented Two-Dot Molecular Quantum Cellular Automata

Hua Qi,[†] Sharad Sharma,[‡] Zhaohui Li,[†] Gregory L. Snider,*[,‡] Alexei O. Orlov,[‡] Craig S. Lent,[‡] and Thomas P. Fehlner*[,†]

Contribution from the Department of Chemistry & Biochemistry and Department of Electrical Engineering, University of Notre Dame, Notre Dame, Indiana 46556-5670

Received July 10, 2003; E-mail: fehlner.1@nd.edu; snider.7@nd.ed

Abstract: The amine functionality of the linker on the dinuclear complex [*trans*-Ru(dppm)$_2$(C≡CFc)(NCCH$_2$-CH$_2$NH$_2$)][PF$_6$] reacts with Si−Cl bonds of a chlorinated, highly B doped Si (111) surface to yield Si−N surface-complex bonds. The surface bound complex is constrained to a near vertical orientation by the chain length of the linker as confirmed by variable angle XPS. Oxidation of the dinuclear complex with ferrocenium ion or electrochemically generates a stable, biased Fe^{III}−Ru^{II} mixed-valence complex on the surface. Characterization of the array of surface bound complexes with spectroscopic as well as electrochemical techniques confirms the presence of strongly bound, chemically robust, mixed-valence complexes. Capping the flat array of complexes with a minimally perturbing mercury electrode permits the equalization of the Fe and Ru energy wells by an applied electric field. The differential capacitance of oxidized and unoxidized bound complexes is compared as a function of voltage applied between the Hg gate and the Si. The results show that electron exchange between the Fe and Ru sites of the array of dinuclear mixed-valence complexes at energy equalization generates a fluctuating dipole that produces a maximum in the capacitance versus voltage curve for each complex-counterion combination present. Passage through the capacitance maximum corresponds to switching of the molecular quantum cellular automata (QCA) cell array by the electric field from the Fe^{III}−Ru^{II} configuration to the Fe^{II}−Ru^{III} configuration, thereby confirming that molecules possess an essential property necessary for their use as elements of a QCA device.

Quantum cellular automata (QCA) constitute a new paradigm for the design of electronic devices in which information stored in structured charge containers is transmitted via coupled electric fields rather than electron currents.[1,2] Decreased resistive heating permits device densities that are higher than those possible with a transistor paradigm. The principles of QCA have been developed theoretically and the essential features of the method have been demonstrated experimentally albeit at near 0 K.[3] To operate, the state energy difference must be greater than *kT*, and, with the 50 nm scale dots and tunnel junctions used in the experiments, extreme low temperature is required. However, state energy difference scales inversely with size, and molecule-sized QCA devices are predicted to operate at room temperature. Hence, we seek to develop molecular QCA cells as an alternative to other contemporary approaches to molecular electronics.[4−7]

A QCA cell containing two quantum dots becomes a mixed-valence complex when scaled to molecular sizes. Mixed-valence complexes have been extensively studied, and many are available.[8−10] Theoretical studies support the applicability of dinuclear mixed-valence complexes to QCA at the molecular level.[11,12] However, there are a number of additional practical requirements a mixed-valence complex must meet to be suitable for use in molecular QCA. Pure compounds in the mixed-valence state and functionalized for surface binding must be available. Oriented surface attachment without loss of necessary mixed-valence properties also must be demonstrated.

We have adopted a stepwise approached to the development of a functional molecular QCA cell. Thus, the foundations upon which the present study is based have already been reported.[13,14]

[†] Department of Chemistry & Biochemistry.
[‡] Department of Electrical Engineering.

(1) Lent, C. S.; Tougaw, P. D.; Porod, W.; Bernstein, G. H. *Nanotechnology* **1993**, *4*, 49.
(2) Lent, C. S. *Science* **2000**, *288*, 1597.
(3) Orlov, A. O.; Amlani, I.; Bernstein, G. H.; Lent, C. S.; Snider, G. L. *Science* **1997**, *277*, 928.
(4) Jacoby, M. *Chem. Eng. News* **2002**, Vol. 80, p 38.
(5) Tour, J. M.; Kozaki, M.; Seminario, J. M. *J. Am. Chem. Soc.* **1998**, *120*, 8486.
(6) Wong, E. W.; Collier, C. P.; Behloradsky, M.; Raymo, F. M.; Stoddart, J. F.; Heath, J. R. *J. Am. Chem. Soc.* **2000**, *122*, 5831.
(7) Fan, F.-R. F.; Yang, J.; Cai, L.; Price, D. W., Jr.; Dirk, S. M.; Kosynkin, D. V.; Yao, Y.; Rawlett, A. M.; Tour, J. M.; Bard, A. J. *J. Am. Chem. Soc.* **2002**, *124*, 5550.
(8) Creutz, C.; Taube, H. *J. Am. Chem. Soc.* **1969**, *91*, 3988.
(9) Ward, M. D. *Chem. Soc. Rev.* **1995**, 121.
(10) Demadis, K. D.; Hartshorn, C. M.; Meyer, T. J. *Chem. Rev.* **2001**, *101*, 2655.
(11) Braun-Sand, S. B.; Wiest, O. *J. Phys. Chem. A* **2003**, *107*, 285.
(12) Lent, C. S.; Isakaen, B.; Lieberman, M. *J. Am. Chem. Soc.* **2003**, *125*, 1056.

10.1021/ja0371909 CCC: $25.00

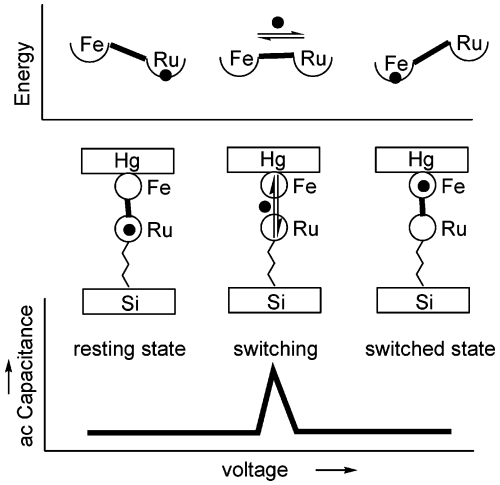

Figure 1. Schematic representation of the experiment showing, from the top, the relative energies of the Fe and Ru wells, the parallel plate capacitor containing the mixed-valence complex, and the capacitance as a function of the voltage imposed across the Hg and Si plates.

A known unsymmetrical mixed-valence complex *trans*-Ru(dppm)$_2$(C≡CFc)Cl, dppm = methylbis(diphenylphosphane), Fc = (η^5-C_5H_5)Fe(η^5-C_5H_4),[15,16] was converted into [*trans*-Ru(dppm)$_2$(C≡CFc)(NCCH$_2$CH$_2$NH$_2$)][PF$_6$], **1**[PF$_6$], which contains a silicon surface binding linker.[13] Both the Fe(II)−Ru(II) and the Fe(III)−Ru(II) cations can be isolated as pure compounds for both derivatives. XPS, XRD structures, solvent effects on near-IR spectra, and substituent effects on redox properties show that both the chloro complex and the complex functionalized for surface binding exhibit type II mixed-valence behavior suitable for QCA applications; that is, addition of the surface connector to the complex does not cause a major change in the mixed-valence properties of the complex. Perturbation of the complex by surface binding was studied on a gold electrode using electrochemical techniques. This work established the basic redox properties of the surface bound **1** were suitable for our application and also demonstrated the robust nature of films of **1**, for example, unchanged electrochemical activity after 1 month in air. In addition, the conditions under which the mixed-valence complex is stable on the surface were defined, and generation of the mixed-valence complex by chemical oxidation of surface bound **1** by [FcH][PF$_6$] was demonstrated.

The next logical step in the development of molecular QCA is to demonstrate switching of the cell (dinuclear mixed-valence metal complex) between states ($Ru^{II}Fe^{III}$ vs $Ru^{III}Fe^{II}$) by an electric field. To accomplish this task, we have created an assembly of biased, vertically oriented, two-dot cells sandwiched between two electrodes and have measured the capacitance of the parallel plate device as a function of applied voltage across the plates. The schematic outline of the experiment is shown in Figure 1. The cells are covalently bound to a semiconductor substrate in a monolayer film, and, to minimize perturbation of the two-dot cells, elemental Hg was chosen for the top electrode. Mercury electrodes are versatile and cause little perturbation of the molecular layer.[17,18] A recent study has emphasized the benefits of Hg junctions for investigating the electrical properties of monolayers on Si.[19] An important feature of the experimental design is the incorporation of a control experiment. Comparative measurements of the capacitive behavior of an array of inactive QCA cells ($Fe^{II}-Ru^{II}$) with that of an equivalent array of active QCA cells ($Fe^{III}-Ru^{II}$) are used to seek evidence for field driven switching. Artifacts associated with features of the film unrelated to electron motion between the Fe and Ru sites versus those associated with switching of the mixed-valence complex are thus differentiated. Related films have been investigated in terms of properties useful for nanoscale devices requiring passage of current for operation.[20,21] These both provide insight as well as describe some limitations of films bound to semiconductor substrates when significant currents are passed.[17,22,23]

Capacitance per unit area, C, is defined as $C = dQ(V)/dV$, where dQ is the change in charge per unit area as a result of an applied ac voltage dV, which can change as a function of the applied dc voltage V. When an electron switches from the Ru to Fe atom, a dipole is created between the moving electron and the stationary counterion. This causes an increase in the measured capacitance at the dc voltage where the dipole is created and destroyed in response to the small ac voltage. As the applied dc voltage is further increased, the stable dipole no longer contributes to the capacitance. As the dipole is created, the dQ measured by the capacitance meter responds to this additional charge, and the measured capacitance becomes $C = C(V) + \{d_1 e \Delta\sigma_m(V)/d_m\}/dV$, where the first term on the right-hand side is the capacitance without the dipole, and the second term represents the additional capacitance due to the dipole formation. $\Delta\sigma_m(V)$ is the change in the dipole charge induced by dV at the applied dc voltage V, d_1 is the distance the electron moves between the Ru and Fe atoms, d_m is the distance between the silicon surface and the mercury surface, (the length of the molecule), and e is the electron charge. Ideally all of the dipoles will form at a certain applied voltage V_o, and $\Delta\sigma_m(V)$ will be a Δ function at V_o; yet due to variations in the molecules and local surface characteristics, there will be some variation in the voltage where the dipole forms. The height of the peak seen in the capacitance measurement depends on the number of molecules per unit area and the width of the voltage distribution of $\Delta\sigma_m$. The narrower the distribution in voltage, the higher the capacitance peak will be. By examining the capacitance data, we can estimate the number molecules per unit area that form dipoles. The integral of the capacitance peak will be the charge $Q = d_1 e \sigma_m/d_m$, which permits the total areal density of dipoles formed to be calculated. This calculated number can then be compared with the density of complexes obtained from independent measurements.

A schematic of the measuring device is shown in Figure 2. Measurements were carried out at 1 MHz using a mercury probe.

(13) Li, Z.; Beatty, A. M.; Fehlner, T. P. *Inorg. Chem.* **2003**, *42*, 5707.
(14) Li, Z.; Fehlner, T. P. *Inorg. Chem.* **2003**, *42*, 5715.
(15) Colbert, M. C. B.; Ingham, S. L.; Lewis, J.; Long, N. J.; Raithby, P. R. *J. Chem. Soc., Dalton Trans.* **1994**, 2215.
(16) Colbert, M. C. B.; Lewis, J.; Long, N. J.; Raithby, P. R.; White, A. J. P.; Williams, D. J. *J. Chem. Soc., Dalton Trans.* **1997**, 99.
(17) Selzer, Y.; Salomon, A.; Ghabboun, J.; Cahen, D. *Angew. Chem., Int. Ed.* **2002**, *41*, 827.
(18) Selzer, Y.; Salomon, A.; Cahen, D. *J. Am. Chem. Soc.* **2002**, *124*, 2886.
(19) Liu, Y.-J.; Yu, H.-Z. *ChemPhysChem* **2002**, 799.
(20) Ashkenasy, G.; Cahen, D.; Cohen, R.; Shanzer, A.; Vilan, A. *Acc. Chem. Res.* **2002**, *35*, 121.
(21) Adams, D. M.; Brus, L.; Chidsey, C. E. D.; Creager, S. E.; Creutz, C.; Kagan, C. R.; Kamat, P. V.; Lieberman, M.; Lindsay, S.; Marcus, R. A.; Metzger, R. M.; Michel-Beyerle, M. E.; Miller, J. R.; Newton, M. D.; Rolison, D. R.; Sankey, O.; Schanze, K. S.; Yardley, J.; Zhu, X. *J. Phys. Chem. B* **2003**, *107*, 6668.
(22) Lin, C.; Kagan, C. R. *J. Am. Chem. Soc.* **2003**, *125*, 336.
(23) Kagan, C. R.; Afzali, A.; Martel, R.; Gignac, L. M.; Solomon, P. M.; Schrott, A. G.; Ek, B. *Nano Lett.* **2003**, *3*, 119.

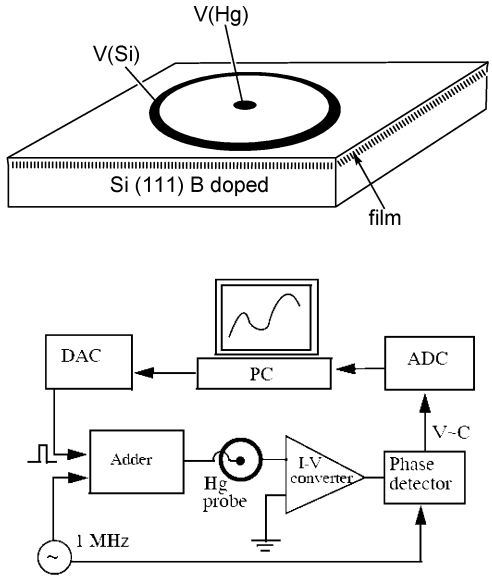

Figure 2. Representation of the Hg contacts to the film of **1** (top) and the gated measuring circuit (bottom).

The method has the advantage of not only being nondestructive but moveable; that is, several areas (0.20 mm^2 each) on a 1.2 cm^2 sample can be measured. A highly doped Si(111) wafer with a dense array of two dot cells oriented perpendicular to the Si surface is tightly held against two fresh Hg surfaces by drawing a vacuum between the probe face and the Si surface. The small axial dot constitutes the upper electrode, whereas larger conductivity associated with the larger area of the annular ring generates effective electrical contact with the semiconductor substrate. The differential capacitance was measured at 1 MHz using a small-signal excitation technique (Sula Technologies capacitance meter). An applied field is varied to equalize the energies of the two metal sites. Under these conditions, the fluctuating dipole generated when the electron moves between the two metal sites leads to an increase in differential capacitance. Initial measurements showed that with a slow sweep of the applied potential capacitance changes possibly associated with switching were not reversible and dependent on sample history. Hence, the gated system shown in Figure 2 was set up. With this device, a dc field can be applied for a variable time period, with a variable delay at zero field between pulses, and with capacitance measurements taken during both periods. By varying the time at potential, delay time, and the sign of the potential, it was empirically shown that minimal film perturbation by the imposed dc field was achieved by employing a pulse/counterpulse (+V pulse followed by −V pulse) voltage-stepping mode with a minimal duty time of 4 ms.

Results and Discussion

Preparation of the Film. The design of complex **1**[PF_6] for surface attachment was guided by several considerations. A functional group compatible with the synthetic chemistry of the basic dinuclear complex of **1** was required. This group must bind strongly to a substrate surface and be resistant to rupture under oxidizing potentials. Convenient rates under mild conditions and good coverages were also highly desirable. The popular thiol-gold surface attachment method was ruled out for two reasons. Capacitance measurements on **1**[PF_6] bound to a gold surface failed using the mercury probe, and the gold-thiol link is susceptible to degradation at modest oxidizing potential. Covalent attachment is more robust, and we considered hydrosilation of alkenes,[24] silylation to form Si−O−Si links,[25] and the reaction of amines with chlorinated Si surfaces.[26,27] The last was compatible with our requirements, and functionalization of the complex was accessible from commercially available reagents. Hence, as already described, **1**[PF_6] was synthesized and fully characterized in preparation for surface attachment.[13]

Table 1. XPS Element Binding Energies (eV) of Si−OH, Si−H, Si−Cl, Si−$\mathbf{1}^+$, and Si−$[\mathbf{1}]^{2+}$ on Highly Doped Si(111) and Ellipsometric Thicknesses (Å)

elements	Si–OH	Si–H	Si–Cl	Si-monolayer (unoxidized)	Si-monolayer (oxidized)
Si 2p	99.3	99.3	99.3	99.3	99.3
SiO 2p	103.4		103.8	103.2	103.2
Cl 2p			200.3, 201.6	199.9, 202.1	199.8, 202.3
N 1s				400.3	400.3
Fe 2p				711.1, 723.9	711.2, 724.2
Ru 3p				462.3, 484.4	462.5, 484.8
P 2p				132.3, 134.7	132.6, 134.8
F 1s				*b*	685.9
thickness	13.9 ± 0.5	1.5 ± 0.5	*a*	17 ± 2	25 ± 5

[a] Too reactive to measure. [b] No signal observed after sonication.

The reaction of a primary amine with a Si−Cl-terminated surface generates a strong Si−N covalent link to the surface; however, the chemistry associated with surface preparation requires several steps, each of which could cause a problem. Hence, insofar as possible, each step in the process was monitored by ellipsometry and XPS (Table 1). The final film was then characterized more extensively, as described in the following two sections, before the capacitance measurements were carried out.

Representative XPS spectra are shown in Figure 3, and AFM measurements are shown in Figure 4. XPS analysis of the clean Si wafer with a thin oxide covering showed no measurable levels of the elements used to define the presence of $\mathbf{1}^+$. AFM on a cleaned and oxidized Si surface gave a rms surface roughness of 0.166 nm (1.0 μm × 1.0 μm). Generation of the H-terminated surface was demonstrated by loss of the SiO signal and a sharp reduction in surface layer thickness. Formation of the Cl-terminated surface was demonstrated by a strong Cl signal accompanied by a small amount of oxide probably formed during sample transfer of this reactive wafer to the XPS chamber.

Reaction with **1**[PF_6] is shown schematically in Figure 5, and the amount of $\mathbf{1}^+$ bound to the surface as a function of reaction time was monitored by electrochemistry (see below) and is shown in Figure 6. Saturation is achieved in 30 h. In most cases, the remaining Si−Cl bonds are then hydrolyzed with water; however, as will be seen below, this step caused a complication. Hydrolysis turned out to be unnecessary and was later left out of the preparative procedure. Successful reaction is also shown by an increase in film thickness to a value close to the known length of $\mathbf{1}^+$ and the appearance of signals in the XPS for the elements found in $\mathbf{1}^+$. The rms surface roughness is 0.194 nm (1.0 μm × 1.0 μm), which is modestly larger that that found for the clean oxide. Unexpectedly, a very weak F signal was

(24) Buriak, J. M.; Allen, M. J. *J. Am. Chem. Soc.* **1998**, *120*, 1339.
(25) Katz, H. E.; Schilling, M. L.; Chidsey, C. E. D.; Putvinski, T. M.; Hutton, R. S. *Chem. Mater.* **1991**, *3*, 699.
(26) Bergerson, W. F.; Mulder, J. A.; Hsung, R. P.; Zhu, X.-Y. *J. Am. Chem. Soc.* **1999**, *121*, 454.
(27) Zhu, X.-Y.; Mulder, J. A.; Bergerson, W. F. *Langmuir* **1999**, *15*, 8147.

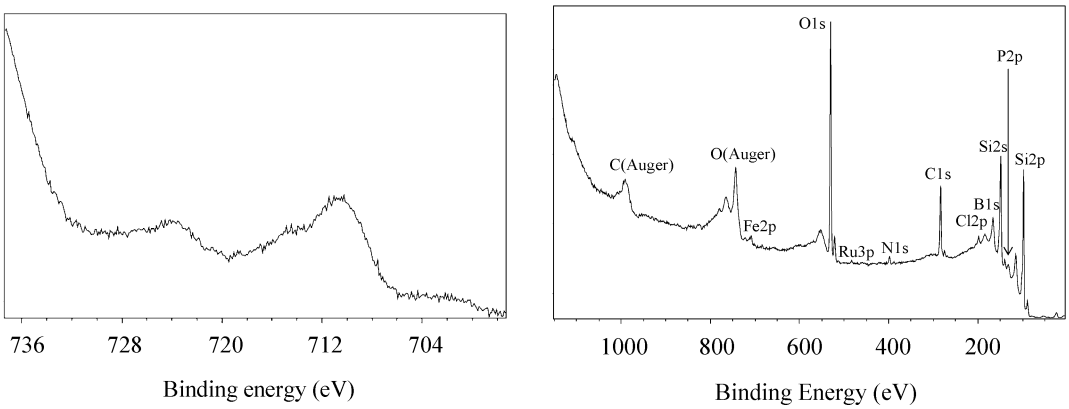

Figure 3. XPS spectra of $\mathbf{1}^+$ bound to a Si(111) surface. Left, Fe(2p); right, survey.

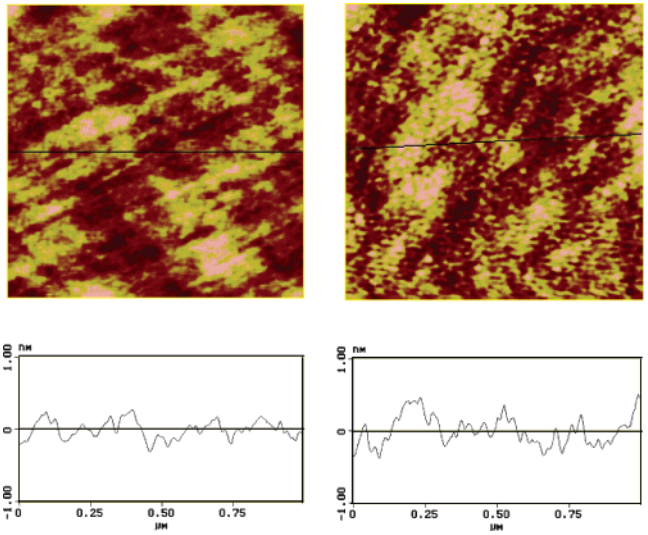

Figure 4. Tapping mode AFM images (left, Si−O surface without film; right, with film of $\mathbf{1}^+$ on the surface).

observed by XPS. This weak F signal was completely removed by sonication in CH_2Cl_2. Clearly the $[PF_6]^-$ counterion of $\mathbf{1}^+$ has been lost. Metathesis with $[Cl]^-$, produced during the surface binding chemistry, constitutes one possible explanation (about 1−2 atom % of Cl is present); however, XPS of a Si−Cl surface without $\mathbf{1}^+$ after hydrolysis also yields a residual Cl signal of about the same intensity. It has been observed previously that treatment of a silica surface with the PF_6 salt of the Creutz−Taube ion leads to loss of the mobile counterion on washing.[28] Presumably, the small amount of HPF_6 present at equilibrium is washed away, driving the acid base equilibrium to produce surface Si−O$^-$ conjugate base sites which serve as the counterions. Hence, we conclude that the counterion of each bound $\mathbf{1}^+$ is a surface Si−O$^-$ site. Vigorous washing, including sonication, does not result in the removal of $\mathbf{1}^+$ from the surface. To produce the active, mixed-valence complex, surface bound $\mathbf{1}^+$ is chemically oxidized with the ferrocenium ion, $[FcH][PF_6]$, and the resulting ferrocene is washed away. Now F is clearly observed in the XPS; however, the intensity of the signal decreases by about a factor of 3 with increased washing times. Thus, in the case of the oxidized complex, we suggest two surface species exist: $[\mathbf{1}][Si{-}O][PF_6]$ and $[\mathbf{1}][Si{-}O]_2$, with the latter becoming the predominant one on extensive washing.

Structure of the Film. For a differential effect of the applied field on the Fe and Ru sites, the molecular two-dot cells must be bound to the surface in a uniform manner and be oriented perpendicular to the plane of the surface with the molecular dipoles in the same direction. Uniformity and near perpendicular orientation is supported by four observations.

The XRD structure of $\mathbf{1}[PF_6]$, the structure of bulk Si, and a molecular model for the NSi_2 bonding[29] are used to model the surface complex. After the H atoms on the amine terminus of the linker were removed, $\mathbf{1}^+$ was docked to a (111) slice of bulk Si representing the surface. Generous N−Si distances were used (2.4 Å, sum of covalent radii = 1.92 Å) to bond to a pair of surface Si atoms with a separation of 3.8 Å, giving a Si−N−Si angle of 106°. The result is shown in Figure 7 as both cylinder and space-filling models. Clearly, even with long N−Si distances, there is near "touching" of the van der Waals radii of the phenyl groups of the dppm ligands with the surface Si atoms. Addition of −OH groups to the adjacent Si atoms will add support to the vertical orientation of surface bound $\mathbf{1}^+$. Other possible variations exist, for example, choice of Si atoms for attachment, but the conclusion remains the same.

Variable angle XPS provides strong evidence of perpendicular orientation of $\mathbf{1}^+$ on the surface. The photoelectron intensity depends exponentially on the distance from the surface of the material analyzed. With some simplifying assumptions, it has been shown that the slope of a plot of $\ln\{[I_x(\theta)/KI_{Si}(\theta)] + 1\}$ versus $1/\sin\theta$ is equal to d/λ, where $I_x(\theta)$ is the intensity of element x at takeoff angle θ, K is a constant (0.6 has been used previously),[30] d is the distance of atom x from the Si substrate, and λ is the inelastic mean free path in Si.[31] As fully dense films have not been achieved and various values of λ have been used in previous studies, the data for the representative elements of $\mathbf{1}^+$ are not used to obtain absolute distances. However, the relative values of the slopes definitively order the elements in terms of height from the Si surface. Typical data and a schematic of the relative distances of the pertinent atomic constituents of $\mathbf{1}^+$ and $\mathbf{1}^{2+}$ from the silicon substrate are shown in Figure 8. The Fe center is above the Ru center, verifying vertical orientation. In addition, the $[PF_6]^-$ counterion of the oxidized material lies between the two metal centers similar to the positioning in the solid-state structure of $\mathbf{1}[PF_6]$.[13] The difference

(28) Wang, Y. *Chemistry & Biochemistry*; University of Notre Dame: Notre Dame, IN, 2002.
(29) Engelhardt, L. M.; Raston, C. L.; White, A. H. *Aust. J. Chem.* **1985**, *38*, 1729.
(30) Huang, X.; Huang, H.; Wu, N.; Hu, R.; Zhu, T.; Liu, Z. *Surf. Sci.* **2000**, *459*, 183.
(31) Fadley, C. S. *Prog. Surf. Sci.* **1984**, *16*, 275.

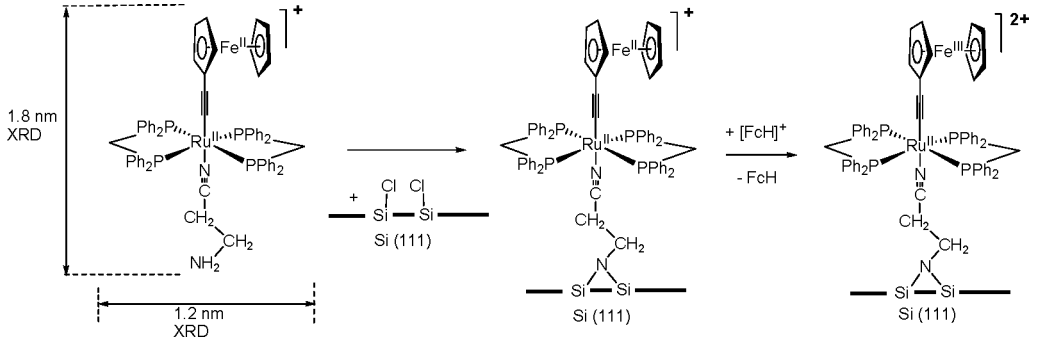

Figure 5. Reaction of **1**[PF_6] with a chlorinated Si(111) surface to produce surface bound $\mathbf{1}^+$ and, subsequently, the mixed-valence state.

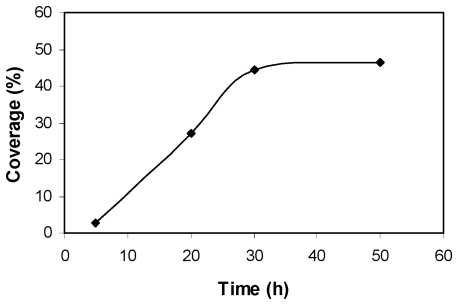

Figure 6. Dependence of surface coverage of $\mathbf{1}^+$ as a function of the deposition time from a 1 mM solution of **1**[PF_6] in CH_2Cl_2.

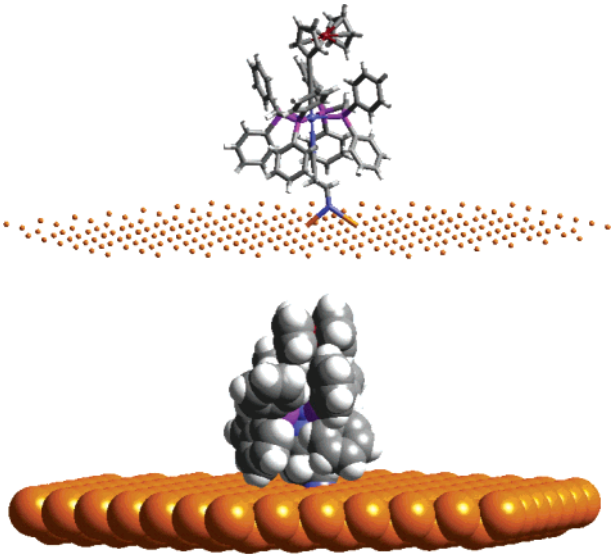

Figure 7. Cylindrical (top) and space-filling (bottom) representations of the docking experiments of $\mathbf{1}^+$ to a Si(111) surface showing a vertical orientation supported by the phenyl groups of the dppm ligands resting on the Si surface atoms.

in the Fe−Ru distances reflects the experimental uncertainty of the measurements.

Two additional observations are consistent with this conclusion. An average of 10 ellipsometry measurements on several unoxidized samples yields a mean film thickness of 17 ± 2 Å, closer to the height of **1**[PF_6] (18 Å), derived from the X-ray diffraction study, than its width (12 Å). In addition, the AFM measurements (Figure 4) of roughness before and after film deposition show that overall roughness has not significantly increased, corroborating uniform coverage of the substrate.

Coverage and Redox Properties of the Film. Electrochemical techniques were used to demonstrate the presence of strongly

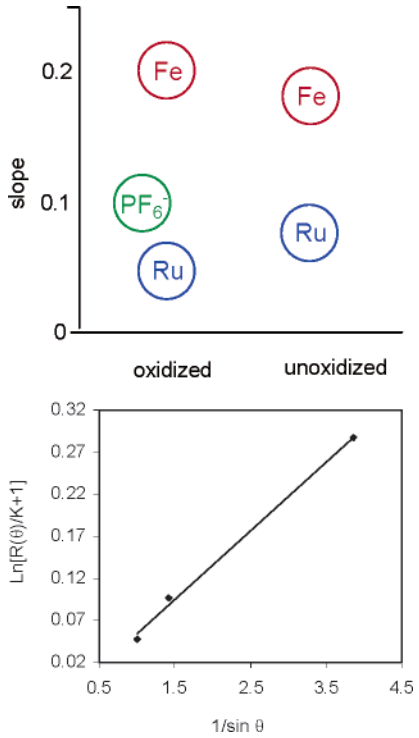

Figure 8. Representation of the variable angle XPS results. Top: plot of the relative positions of the metal centers and anions relative to the Si substrate for oxidized and unoxidized films. Bottom: plot of $\ln[R(\theta)/K + 1]$ versus $1/\sin\theta$ for Ru(3p) ionization, the slope of which is $d(\mathrm{Ru})/\lambda$.

bound redox active centers, the approximate strength of the interaction between the redox centers, the areal coverage of active centers, the extent of chemical oxidation of the film, the order of magnitude rate of electron transfer between the Si electrode and the redox centers, and the integrity of redox activity before and after capacitance measurements.

There is a qualitative difference between the cyclic voltammetric (CV) behavior of a free redox active species in solution and those strongly bound to an electrode surface.[32] If the redox active species is strongly bound to the surface, in a uniform environment, and the rate of electron transfer from electrode to complex is fast, then a single redox process yields anodic and cathodic waves of 91 mV fwhm with the peak maximum of each wave at the same potential. As seen from Figure 9, films of $\mathbf{1}^+$ on Si yield 140 mV fwhm peaks with a splitting of 60 mV. This demonstrates good uniformity and redox centers that interact to a measurable extent. Previous studies have shown

(32) Bard, A. J.; Faulkner, L. R. *Electrochemical Methods*; Wiley: New York, 2001.

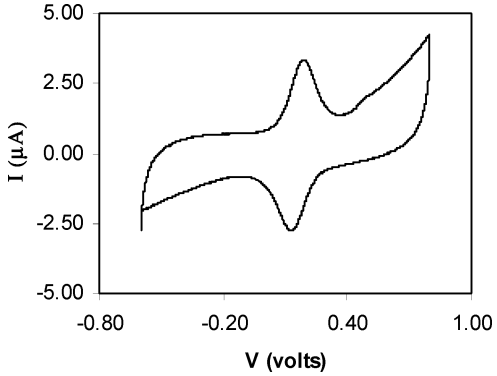

Figure 9. CV of $\mathbf{1}^+$ bound to a highly doped Si surface (10 mV/s, 0.1 M $TBAPF_6$ in CH_2Cl_2).

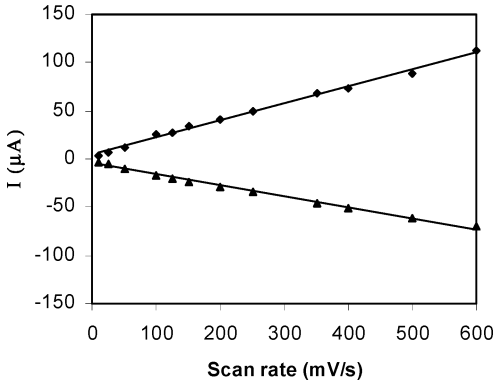

Figure 10. Plot of maximum current versus scan rate for oxidation (◆) and reduction (▲) (0.1 M $TBAPF_6$ in CH_2Cl_2).

very broad waves for strongly interacting surface bound ferrocenes − the interaction is much weaker here.[33] Relative to $\mathbf{1}^+$ bound to a Au surface, the nonzero splitting between the peak maxima at the scan rate shown indicates a lower electrode to complex electron-transfer rate.[14] The area under either of the two waves corresponds to the total charge which, when combined with the surface area of the electrode in the electrolyte, yields an areal density of redox sites of 4×10^{13} cm^{-2} (45% coverage). Substrates with a greater degree of roughness as measured by AFM showed significantly higher apparent coverages, for example, 77% for rms 0.423 nm versus 45% for rms 0.166 nm. Hence, the areal density calculated from the electrochemical measurements is a maximum value.

The functional dependence of peak current on scan rate also qualitatively distinguishes strongly bound redox active complexes from those in solution. As shown in Figure 10, the linear dependence on scan rate is in accord with the equation $i = n^2F^2\upsilon N/4RT$, where n is the number of electrons transferred, F is the faraday constant, υ is the scan rate, N is the number of redox sites, R is the gas constant, and T is the absolute temperature.[32] The slope of the plot and the electrode surface area yield an independent measure of the areal density of redox sites of 3×10^{13} cm^{-2}, in good agreement with the value obtained by integration of the CV wave.

As already mentioned, a nonzero $E_a - E_c$ for the peak maxima suggests the rate of electron transfer from the silicon electrode through the molecular tether to the metal sites is slow enough to perturb the CV measurements.[34−36] The rate of electron

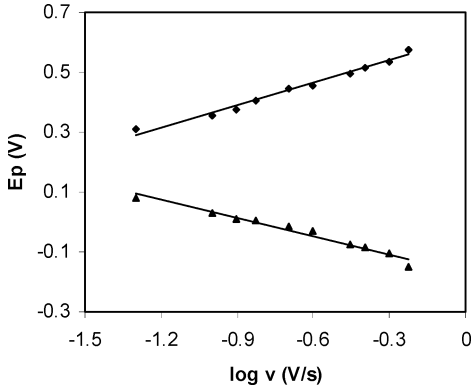

Figure 11. Linear dependence of E_p on the scan rate for $\Delta E_p > 200$ mV (E_{p_a}, ◆; E_{p_c}, ▲).

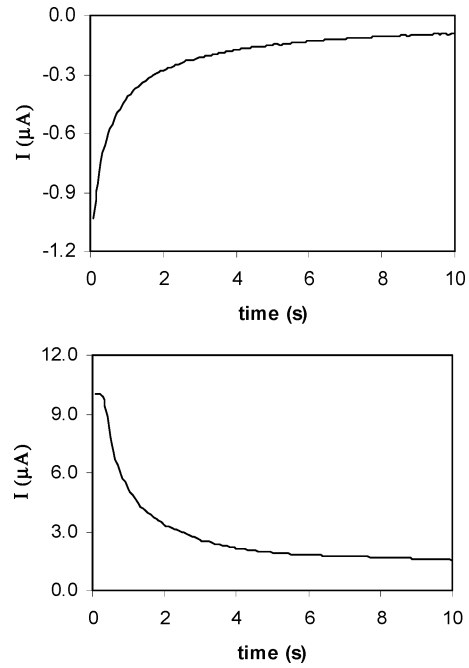

Figure 12. DCPA of a chemically oxidized film of $\mathbf{1}^+$ on silicon at −100 mV (top) and a subsequent DCPA of the same film at 500 mV (bottom). The latter is identical to that observed for an as-prepared film.

transfer between Si and $\mathbf{1}^+$ is $k \approx \alpha nF\upsilon_c/RT = (1 - \alpha)nF\upsilon_a/RT$, where υ_c and υ_a are slopes of plots of E_c and E_a versus log υ (scan rate) and α is a constant for a given system. Provided $\Delta E_p > 200$ mV, p = a, c, the equation $\upsilon_a/\upsilon_c = \alpha/(1 - \alpha)$ holds, and the values of υ_p obtained from the plot of E_p versus log of the scan rate (Figure 11) yield $k \approx 4.3$ s^{-1}, reflecting a slower rate than that for $\mathbf{1}^+$ on a gold surface.[14]

As described above, films of $\mathbf{1}^+$ are chemically oxidized with $[FcH][PF_6]$. To investigate the stability of the mixed-valence films, as well as to estimate the yield of mixed-valence complexes, the films were discharged using a dc potential amperometric (DCPA) technique to measure charging and discharging curves. This approach was used earlier in analyzing the charge state of Au bound films of $\mathbf{1}^+$.[14] As shown in Figure 12, application of a reducing potential demonstrates reduction of the oxidized film, whereas application of an oxidation potential

(33) Auletta, T.; van Veggel, F. C. J. M.; Reinhoudt, D. N. *Langmuir* **2002**, *18*, 1288.
(34) Laviron, E. *J. Electroanal. Chem.* **1979**, *101*, 19.
(35) Chidsey, C. E. D.; Bertozzi, C. R.; Putvinski, T. M.; Mujsce, A. M. *J. Am. Chem. Soc.* **1990**, *112*, 4301.
(36) Weber, K.; Creager, S. E. *Anal. Chem.* **1994**, *66*, 3164.

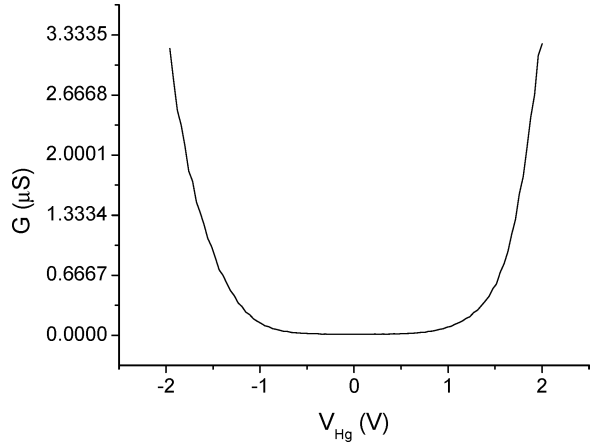

Figure 13. Conductance of a film of $\mathbf{1}^{+}$ on silicon as a function of applied voltage.

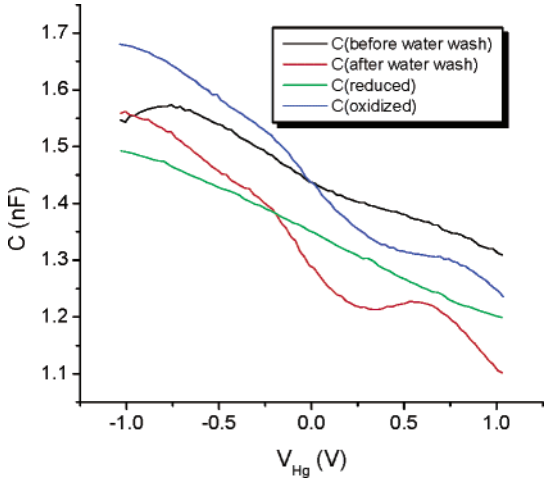

Figure 14. Capacitance of unoxidized $\mathbf{1}^{+}$ on silicon as a function of voltage. Pulse/counterpulse measurements (4 ms on, 800 ms off). Black: as-prepared film without water wash. Red: as-prepared film washed with water wash. Green: as-prepared film with water wash after electrochemical reduction. Blue: as-prepared film with water wash after electrochemical reduction and electrochemical oxidation. The last three are measured with the same sample albeit at different spots. Empirically we observe that an electrochemically oxidized film is more air sensitive than the as-prepared or reduced films. Hence, the lower intensity of the blue curve relative to red is attributed to a lower surface density of mixed-valence $\mathbf{1}^{2+}$.

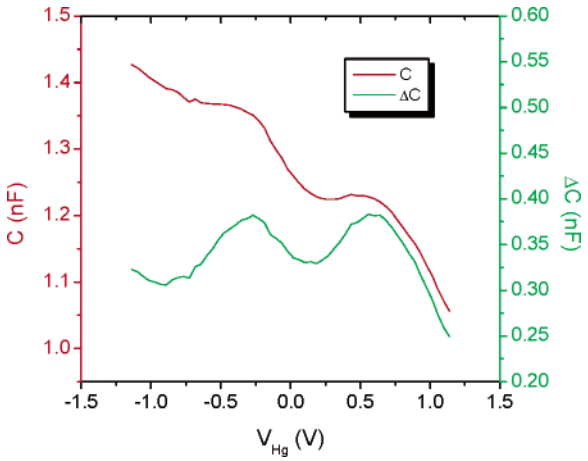

Figure 15. Capacitance of chemically oxidized $\mathbf{1}^{+}$ on silicon as a function of voltage. Pulse/counterpulse measurements (4 ms on, 800 ms off) are in red with the difference (oxidized − electrochemically reduced baseline) in green.

to either an as-prepared film or the discharged film demonstrates oxidation. There is good agreement between the integrated charge from DCPA on unoxidized films and that found under the CV wave. Conventional CV experiments after chemical oxidation demonstrate that the oxidation procedures did not cause degradation of the CV response. It will be noted from Figure 12 that the peak current for reduction of the chemically oxidized film, as well as the integrated charge, is less than that for oxidation of the as-prepared film. The integrated charge is taken as a measure of yield, and in these experiments only 10−20% of the film is oxidized by ferrocenium ion.

Capacitance Measurements. Control Experiments. The film conductance was measured to establish the field strength limits for valid capacitance measurements. The conductance for a typical film is shown in Figure 13, where it is seen that capacitance measurements between +1.2 and −1.2 V are justified. The size of this window changes somewhat between samples and is reduced in size as film roughness increases. To identify capacitance changes associated exclusively with the mixed-valence complex, an unoxidized film serves as the baseline experiment. A single wafer is prepared with bound $\mathbf{1}^{+}$ and is then divided into parts, one of which is chemically oxidized. We discovered by DCPA that the "as-prepared" film which had been washed with water is partially oxidized and shows capacitance maxima (Figure 14, red) which disappear on electrochemical reduction (green) and reappear again on oxidation (blue). If the water wash is omitted, no maxima are observed (black). Possibly residual Cl_2 from the Si−Cl formation step generates the oxidizing agent HOCl on reaction with water. Whatever the cause, the electrochemically reduced film or the "as-prepared" film without water treatment constitutes the baseline capacitance measurement.

The baseline capacitance is ∼1 nF for these films. For a parallel plate capacitor, $C = \epsilon A/d$, where A is the area of the central Hg dot, 2×10^{-3} cm^2, and d is the length of $\mathbf{1}^{+}$, 18 Å. If one uses $\epsilon = 2.6$,[37] the calculated capacitance is 3 nF in acceptable agreement as the appropriate value of ϵ for **1** is not known. Over a 3 V scan range, C varies about 20%. The capacitance during the delay periods is constant (Supporting Information).

After the capacitance measurements, the oxidized, as-prepared, and electrochemically reduced films were analyzed to verify the presence (XPS) of active complexes (CV) and, in the case of the oxidized films, charged complexes (DCPA). In contrast to many surface bound molecular "devices" which cannot be recycling more than a few times,[17,22] the system described here exhibits reproducibility in terms of location on the substrate and repetitive scans. The oxidized (active) surface is modestly air sensitive and degrades with time; however, the unoxidized surface lasts for weeks.

Mixed-Valence Complex. Typical capacitance measurements on a film containing chemically oxidized **1** are shown in Figure 15, where the difference spectrum shows two features of approximately equal intensity at 0.7 and −0.4 V Hg. These new features result from deliberate oxidation of the film and disappear on reduction. Therefore, they can be attributed to the presence of mixed-valence $\mathbf{1}^{2+}$. Measurements at different

(37) Wei, J.; Liu, H.; Dick, A. R.; Yamamoto, H.; He, Y.; Waldeck, D. H. *J. Am. Chem. Soc.* **2002**, *124*, 9591.

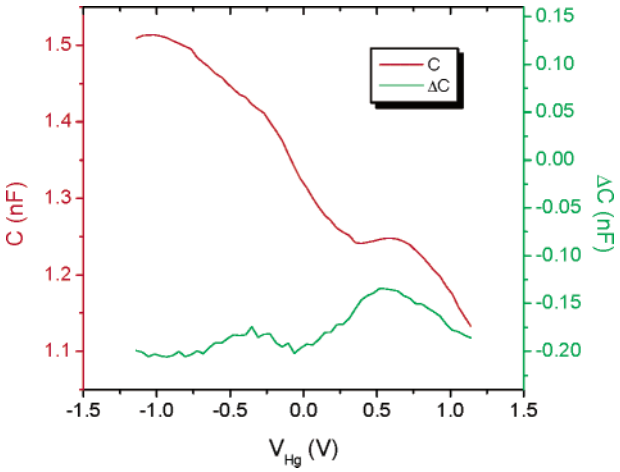

Figure 16. Capacitance of chemically oxidized $\mathbf{1}^{+}$ on silicon as a function of voltage. Pulse/counterpulse measurements (4 ms on, 800 ms off) are in red with the difference in green after increasing the washing time of the oxidized film by a factor of 4.

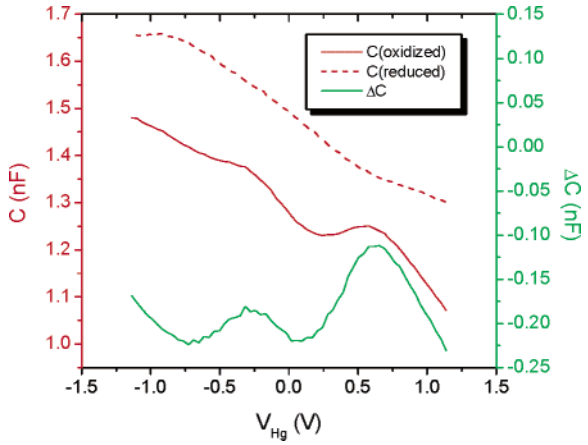

Figure 17. Capacitance of electrochemically oxidized $\mathbf{1}^{+}$ on silicon as a function of voltage. Pulse/counterpulse measurements (4 ms on, 800 ms off) are in red with the difference in green using the electrochemically reduced film as the baseline.

surface positions are internally consistent in that as many as eight observations per sample consistently yielded the capacitance peaks illustrated here. From the charge represented by the capacitance peak at +0.7 V, the distance between the metal centers = 0.6 nm (XRD), the thickness of the film = 2 nm (ellipsometry), the value calculated for σ_m of 8×10^{11} cm^{-2} is in acceptable agreement with the maximum areal density of 3×10^{12} cm^{-2} for $\mathbf{1}^{2+}$ in the chemically oxidized film as measured electrochemically. The enhanced capacitance is attributed to rapid flipping of the dipole associated with the exchange of an electron between the Fe and Ru sites at the potential where metal well energies are equalized, that is, switching of the two-dot QCA cell.

The presence of two signals when one is expected for a single species on the surface is attributed to the existence of two chemically distinct mixed-valence complexes on the silicon substrate, that is, [**1**][Si−O][PF_6] and [**1**][Si−O]$_2$ (see above). One species possesses a mobile anion, whereas the other does not. Hence, to assign the signals as well as corroborate the assignment, a chemically oxidized sample was washed several times more before measurement. The results are shown in Figure 16, where it is seen that the signal at −0.4 V is distinctly reduced relative to the signal at 0.7 V. XPS measurements of F verified a decrease in $[PF_6]^-$. Hence, the signal at −0.4 V is attributed to [**1**][Si−O][PF_6], and the signal at 0.7 V is assigned to [**1**][Si−O]$_2$. Finally, Figure 17 gives results for a film which is electrochemically oxidized with a [$N(Bu)_4$][PF_6] salt as the electrolyte as opposed to chemical oxidation utilizing the ferrocenium PF_6 oxidant. Two different methods of oxidation yield essentially the same results, thereby corroborating the interpretation above.

Simple external field driven equalization of the Fe, Ru well energies requires the capacitance maximum to occur at positive potentials (Figure 1). Unfortunately, the zero of potential within the film is not the same as that of the applied voltage and would be difficult to determine accurately. Hence, we do not consider the sign of the applied potential to give meaningful information. Furthermore, direct field driven switching of the two types of molecular QCA cells is possible as well as indirect mechanisms, for example, ion movement within the film driven by the applied electric field. For anions, this would occur under the opposite potential of direct switching and could only be observed for mobile anions, for example, for [**1**][Si−O][PF_6] observed at −0.4 V. Pertinent to the counterion switching mechanism, small changes in counterion position in the solid state are known to measurably perturb barriers for electron exchange in mixed-valence complexes.[38] Even changes in solvent, often assumed inert, are known to affect observed charge site stability in solvated mixed-valence complexes.[39] A recent theoretical study utilizing a unit point charge as a driver to evaluate the switching characteristics of a molecular mixed-valence complex in the gas phase shows that ion switching is feasible.[12]

Capacitive measurements on a device related to that described here have recently been communicated.[40,41] This device consists of functionalized ferrocene moieties covalently bound to a Si substrate. The top of the film makes electrical contact with a metal electrode via an electrolyte. Both current (CV) and ac capacitance are measured as the voltage between the Si substrate and the metal electrode is varied. Redox behavior characteristic of ferrocene is observed in the CV, and at the potential of the ferrocene/ferrocenium couple a maximum in the capacitance is observed. The maximum capacitance signal is observed at 25 Hz, but at 1 kHz the signal is unobservable. The loss of signal is attributed to rate-limiting electron transfer at the higher frequencies. The kinetics for electron transfer between $\mathbf{1}^{+}$ and the Si electrode, which were measured by CV, rule out this mechanism as an explanation for the observed signals in our experiments. Similarly, it is unlikely that capacitive changes associated with redox processes taking place between the complex and the Hg electrode would be observed at the measuring frequency of 1 MHz. Note that the rate of thermal electron transfer estimated from the energy of the intervalence charge-transfer transition is $\sim 10^7$ s^{-1} and permits response to a 1 MHz field.[8] Finally, if the signals observed in our experiments were due to redox processes rather than electron

(38) Dong, T.-Y.; Schei, C.-C.; Hsu, T.-L.; Lee, S.-L.; Li, S.-J. *Inorg. Chem.* **1991**, *30*, 2457.
(39) Chen, Y. J.; Kao, C.-H.; Lin, S. J.; Tai, C.-C.; Kwan, K. S. *Inorg. Chem.* **2000**, *39*, 189.
(40) Li, Q.; Mathur, G.; Homsi, M.; Surthi, S.; Misra, V.; Malinovskii, V.; Schweikart, K.-H.; Yu, L.; Lindsey, J. S.; Liu, Z.; Dabke, R. B.; Yasseri, A.; Bocian, D. F.; Kuhr, W. G. *Appl. Phys. Lett.* **2002**, *81*, 1494.
(41) Li, Q.; Surthi, S.; Mathur, G.; Gowda, S.; Misra, V.; Sorenson, T. A.; Tenent, R. C.; Kuhr, W. G.; Tamaru, S.; Lindsey, J. S.; Liu, Z.; Bocian, D. F. *Appl. Phys. Lett.* **2003**, *83*, 198.

switching between metal sites, then the signals should be observed for both reduced and oxidized films. This is not the case.

Although many details of the mechanism of the switching observed for $\mathbf{1}^{2+}$ remain to be discovered, these results constitute another step in establishing the feasibility of molecular QCA, an essential feature of which is rapid switching caused by a changing electric field. Among those questions still to be investigated are the differences between the molecular array investigated here and single molecules or lines of molecules; the generation of surface bound, unbiased molecular QCA cells; and the perturbation in switching potential caused by counterion properties. Relative to the last, it is encouraging that effective counterion immobilization by elimination of protonated mobile counterion takes place. However, with surface bound anions, even a symmetrical vertical complex would remain biased. The ideal situation would be a neutral mixed-valence complex. Vertical orientation is not necessary, however, and the four-dot molecular QCA cell recently reported would operate in a horizontal orientation.[42] Despite the many challenges that remain, thus far all of the experimental results support the possible expression of QCA at the molecular scale.

Experimental Section

General. Complex **1**[PF_6] was prepared as described previously.[13] Standard Schlenk line or drybox procedures were employed for chemical transformations involving sensitive materials.[43]

Preparation of Oxidized Silicon and Silicon-Hydride Surface. A slice of a Si (111, B doped, 0.001 Ω cm) wafer with a single side polished was cleaned for 15 min at 80 °C in 4:1:1 H_2O:NH_4OH:H_2O_2, by volume, for 15 min at 80 °C in a 4:1:1 H_2O:HCl:H_2O_2, by volume, and finally for 2 h at ∼100 °C in 3:1 H_2SO_4 (conc):H_2O_2 (30%), by volume. (*Warning: The last cleaning solution, piranha solution, should be handled with caution; it can detonate unexpectedly.*) The wafer was rinsed thoroughly with flowing deionized water between and after each cleaning. To generate the Si−H surface, the oxidized silicon wafer was dried with an inert gas and immersed in nitrogen-purged 40% NH_4F aqueous solution for 4−6 min or a 10% HF solution for 2 min. (*Warning: Chlorine gas and HF are extremely corrosive and must be handled with due precautions.*) These etching conditions have been employed effectively by others.[44−47] The resulting hydrophobic surface was rinsed with flowing water for 30 s, and then dried under argon.

Preparation of Silicon−Chlorine Surface.[26,48] The hydrogen capped silicon wafer was transferred to a Schlenk tube which was connected to a vacuum line pumped by a mechanical pump and evacuated to a base pressure of 5×10^{-2} Torr, and then filled with Cl_2 gas at a temperature of 80 °C. The unreacted chlorine was driven out by inert gas after 20 min and absorbed by sodium iodide solution.

Preparation of Silicon-Complex Surface.[26] A freshly prepared chlorine capped silicon surface was placed into a solution (1 mM) of **1**[PF_6] at room temperature. The sample was then taken out and sequentially washed in methylene chloride, acetone, ethanol, and 18 MΩ cm of water for 2−3 min each to remove the physically adsorbed material and to hydrolyze the residual Si−Cl bonds. It was then dried in a stream of inert gas. The redox properties, as measured by cyclic voltametry, of samples prepared by this method did not change appreciably on storing in air for 1 month. For capacitance measurements, a given sample was divided. One piece was reserved for the baseline measurements, and the other was oxidized with excess [FcH][PF_6] (Aldrich) in methylene chloride by soaking at room temperature for 80 min in a drybox. The oxidized sample was removed and washed with the three solvents for 2 min each and then dried with inert gas. These sample contained the $[PF_6]^-$ counterion (F by XPS); however, washing for 8 min in each of the three solvents led to substantial reduction in the amount of $[PF_6]^-$ ion in the film.

X-ray Photoelectron Spectroscopy (XPS). X-ray photoelectron spectra were obtained on a Kratos XSAM 800 instrument operating with a Mg Kα X-ray source (1253.6 eV). The pressure in the analytical chamber was in the 10^{-8} Torr range. The analysis pass energy was set to 80 eV for survey scans and high resolution scans. Both oxidized and unoxidized samples were examined before and after capacitance measurements. The binding energy scales are referenced to Si 2p (99.3 eV), and spectra were obtained at approximate takeoff angles of 90° from the surface as well as 45° and 15° for the angle resolved data. Spectra of Fe 2p, Ru 3p, N 1s, F 1s, Cl 2p, Si 2p (substrate), and B 1s (dopant) as well as survey scans (1153.6, ∼9.6 eV binding energy) were recorded for each sample.

Monolayer Thickness Measurements. Ellipsometric thickness measurements were carried out on a Dudolph Autoel III using a helium−neon laser light source. A clean Si(100) wafer with native oxidized layer was used as standard reference. The installed ellipsometry programs were used to calculate the film thicknesses. An index of refraction of 1.46 was used in the calculation film thicknesses.

AFM Measurements. Atomic force microscope (AFM) images were obtained with a Dimension 3000 instrument and a Nanoscope III controller (Digital Instruments, Santa Barbara, CA) and were carried out in the air. Data were collected in the tapping mode and analyzed using Digital Instruments software. The n^+-silicon tip with cantilever used here possesses a spring constant $k = 35$ N/m and a fundamental resonance frequency $f = 330$ kHz.

Electrochemical Measurements. Cyclic voltammetric (CV) and dc potential amperometry (DCPA) measurements of the silicon bound complex $\mathbf{1}^+$ were performed on a BAS Epsilon-EC instrument using a Pt-plate counter electrode and a Pt-wire pseudoreference electrode along with the highly doped silicon working electrode. In preparation for this work, the solution and Au surface bound electrochemistry on $\mathbf{1}^+$ have been reported earlier.[13,14] All electrochemical measurements were done at room temperature under an inert atmosphere in a dedicated drybox. Tetrabutylammonium hexafluorophosphate ($TBAPF_6$, Aldrich) at 0.1 M concentration in CH_2Cl_2 solvent was used as the supporting electrolyte.

The charge state of the films was measured by using DCPA techniques. In similar fashion, oxidized and reduced films were made for capacitance measurements to compare with the results from chemical oxidation. For the former, surface bound $\mathbf{1}^+$ was oxidized by application of a potential of 500 mV which was sufficiently high to oxidize the complex but not so high to rapidly degrade it. The silicon electrode was removed from the electrolyte under positive potential. Surface bound molecules were reduced by the application of a reducing potential of −100 mV. CV shows that only 40% of the molecules survived the electrochemical oxidation followed by the capacitance measurements (air exposure for 30 min). This indicates that the electrochemically oxidized sample is less stable than the chemically oxidized sample which survives for a couple of weeks after exposure to air. On the other hand, the electrochemically reduced sample was as stable in the air as was the as-prepared film.

Capacitance Measurements. Capacitance measurements on the films were carried out at 1 MHz using a mercury probe (Hg-412RD-2L, MSI electronics, Inc., Long Island, NY). The wafer is held against the two-contact Hg probe by vacuum. The inner contact is a small dot

(42) Jiao, J.; Long, G. J.; Grandjean, F.; Beatty, A. M.; Fehlner, T. P. *J. Am. Chem. Soc.* **2003**, *125*, 7522.
(43) Shriver, D. F.; Drezdzon, M. A. *The Manipulation of Air-Sensitive Compounds*, 2nd ed.; Wiley-Interscience: New York, 1986.
(44) Linford, M. R.; Fenter, P.; Eisenberger, P. M.; Chidsey, C. E. D. *J. Am. Chem. Soc.* **1995**, *117*, 3145.
(45) Higashi, G. S.; Chabal, Y. J.; Trucks, G. W.; Raghavachari, K. *Appl. Phys. Lett.* **1990**, *56*, 656.
(46) Zhu, X. Y.; Boiadjiev, V.; Mulder, J. A.; Husung, R. P.; Major, R. C. *Langmuir* **2000**, *16*, 6766.
(47) Cicero, R. L.; Linford, M. R.; Chidsey, C. E. D. *Langmuir* **2000**, *16*, 5688.
(48) Jun, Y.; Le, D.; Zhu, X. Y. *Langmuir* **2000**, *16*, 3415.

having an area of 0.2 mm^2 (confirmed by measuring an oxide layer of known thickness) which forms a capacitance between the substrate and a Hg dot, C_1. The outer contact having the shape of an annular ring has a much larger area (6.4 mm^2, see Figure 2). Because of its large area, the outer contact has 32 times larger capacitance C_2 to the wafer as compared to the C_1. Because the C_1 and C_2 are in series through the highly doped substrate, the total capacitance seen between the two contacts is dominated by the smaller capacitance ($C_{total} = C_1C_2/(C_1 + C_2) \approx C_1$ with an accuracy of 97%).

Differential capacitance is measured at 1 MHz with an excitation signal of 50 mV using a capacitance meter from Sula Technologies. The system incorporates the adder, the phase detector, and the signal generator as shown in Figure 2. The capacitance meter is interfaced with a PC through a 6024E DAQ (Analogue Input/Output Board) from National Instruments. The digital to analogue converter (DAC) is used to produce pulses applied to the sample; the signal from the capacitance meter is acquired by an analogue to digital converter (ADC). The waveform parameters such as pulse width, delay, etc. can be conveniently controlled using the software with an accuracy of about 1 ms.

After the measurement was completed, the vacuum that sustains the Hg contact is removed, breaking the Hg-wafer surface contact. The Hg is returned to the reservoir through the siphon tube, providing a fresh Hg surface for each measurement. Multiple positions on the samples (area of 1.2 cm^2) are examined for each wafer to confirm reproducibility.

Acknowledgment. We thank Professor M. Lieberman for assistance with the ellipsometry and helpful discussions, Dr B. Varughese for assistance with the XPS experiments, Dr. A. M. Beatty for the modeling of the complex on the surface, Dr. M. Thoms for aid with the synthesis, and Professor D. Meisel for access to the AFM instrument. A grant from ONR/DARPA (N00014-00-1-0746) is gratefully acknowledged.

Supporting Information Available: Complete capacitance measurements (pulse, counterpulse, and delay periods) for four different samples oxidized (activated) by electrochemical or chemical means (PDF). This material is available free of charge via the Internet at http://pubs.acs.org.

JA0371909